Supporting Information

Elastic strain-hardening and shear-thickening exhibited by thermoreversible physical hydrogels based on poly(alkylene oxide)-grafted hyaluronic acid or carboxymethylcellulose

Markus L. Andersson Trojer[a,b,1], Mats Andersson[c,d], Johan Bergenholtz[e], Paul Gatenholm[f]

[a]Department of Colloid Chemistry, Interactions in Complex Monolayers, Max Planck Institute of Colloids and Interfaces, DE-14476 Potsdam, Germany.

[b]Department of Chemistry, Biomaterials and Textiles, Fibre Development, RISE IVF, Mölndal, Sweden.

[c]Department of Chemistry and Chemical Engineering, Polymer Technology, Chalmers University of Technology, SE-41296 Göteborg, Sweden.

[d]Institute for NanoScale Science & Technology, Flinders University, Bedford Park, Adelaide, South Australia 5042, Australia.

[e]Department of Chemistry and Molecular Biology, University of Gothenburg,SE-412 96 Göteborg, Sweden.

[f]Department of Chemistry and Chemical Engineering, Biopolymer Technology, Chalmers University of Technology, SE-41296 Göteborg, Sweden.

1 Corresponding author. E-mail: markus.andersson-trojer@ri.se. Telephone: +46 10-516 50 00

1 Contents

1.1 List of Figures

1.2 List of Tables

2 Quantitative coupling and characterization

Sodium hyaluronate (100 000 g/mol) obtained by fermentation of *Bacillus subtillis* was kindly provided by Mr. Kristoffer Tømmeraas (Novozymes Biopolymers A/S, Bagsvaerd, DK). Sodium carboxymethylcellulose, Cekol 30 (100 000 g/mol) with a DS of 0,75 was gently offered by Göran Kloow (CP Kelco AB, Skoghall, Sweden). EDC (SigmaUltra) and NHS (98 % Aldrich) were both chemicals purchased from Sigma-Aldrich (Steinheim, DE).

Figure 2.1. Material and chemical setup for synthesis.

The PAOs were provided by Dr. Katty Darragas (Huntsman, Everberg, Belgium), and are listed in Table S2.1. The molecular weight of the PAOs was characterized using Maldi-TOF (see Section 2.2.2) and the molecular structure was characterized using NMR (see Section 2.2.4).

Table S2.1. Physical properties of polysaccharide and polyether prepolymers.

	Polyethers					Polysaccharides		
	M_n [kg/mol][a]	PDI[a]	EO:PO[b]	End groups		M_w [kg/mol][c]	PDI[c]	DS[d]
$M^{NH_2}600$	0.60	1.03	2:12	CH_3-, -NH_2	CMC[1]	100	2.2	0.75
$M^{NH_2}2005$	2.00	1.03	5:30	CH_3-, -NH_2	HA	100	1.8	

[a]MALDI-TOF (see Section 2.2.2). [b]NMR. [c]SEC-MALLS. [d]Data from supplier.

2.1 Quantitative coupling

The synthetic route and the characterization of the resulting graft copolymers has been described in detail in a previous work[1]. The PSas (100 mL, 1 wt%) and PAOs (10 mL with different concentrations depending on the desired grafting ratio) were dissolved separately in a three necked flask and beaker respectively under vigorously stirring for one day and then mixed. A probe sample (5 mL) for SEC-analysis was taken after 15 min. To compensate the hydrophobicity of PO-dominated PAOs, these reactions were allowed to proceed under cooling in an icebath. NHS was added to the reaction medium under stirring, and pH was adjusted to 8 with 0.1 M NaOH. At last, EDC was added to the solution and pH was maintained at 8 with addition of 0.1 M HCl. EDC and NHS was added in excess with the optimized molar ratios; [EDC]:[NHS]:[-NH_2]=15:7.5:1. The reaction was allowed to proceed overnight. Before purification, the pH was readjusted to 7 with 0.1 M HCl. The total reaction volume was measured and a 5 mL probe sample was taken for SEC measurements. The product was purified with dialysis (Spectra/Por 2, regenerated cellulose MWCO 12-14 000 g/mol) against distilled water during three days and finally freeze dried at -52 °C for three days in a Heto Powerdry PL3000 (Heto Lab equipment, Allerød) equipped with an Edwards RV5 vacuum pump and a HETO HSC 500 temperature controller. The samples were sealed with perforated alufoil.

2.2 Characterization

In the following sub-sections, the tools used for characterization are described and the results are presented for the example graft copolymers PSa-(g-$M^{NH_2}2005$)$_{5.0\%}$. For the full details of the synthetic route and characterization of the entire range of graft copolymers synthesized, the reader is referred to our previous work[1].

2.2.1 Size exclusion chromatography

The molecular weight of the polysaccharide and polyether prepolymers was determined by SEC on a Waters 2690 instrument (Waters Corporation) with online MALLS (Dawn DSP equipped with an HE_NE laser at 632.8 nm, Wyatt Technology corp., Santa Barbara, CA, USA) and RI detector (Optilab DSP, Wyatt Technology corp., Santa Barbara, CA, USA). For analysis of hydrophilic polyethers as well as polysaccharides, the columns (three serial connected columns; Shodex OHpak SB-803 HQ, SB-804 HQ and SB-806M HQ) were controlled at 50°C. Regarding hydrophobic PAOs, the temperature was controlled at 25°C. Furthermore, the system had an online degasser, autosampler and a column oven. The eluent was 0.1M sodium nitrate ($NaNO_3$) with 0.02% sodium azide (NaN_3). All samples were prepared as 2 wt% solution in MilliQ water.

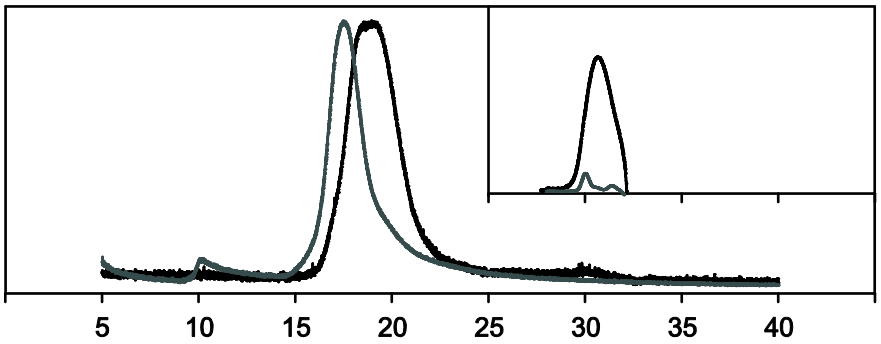

Figure S2.2. LS signals of CMC (black) from the reaction mixture before the coupling and CMC-(*g*-$M^{NH_2}2005)_{5\%}$ (grey). The inset displays the RI signal in the PAO region of the reaction mixture before and after the coupling.

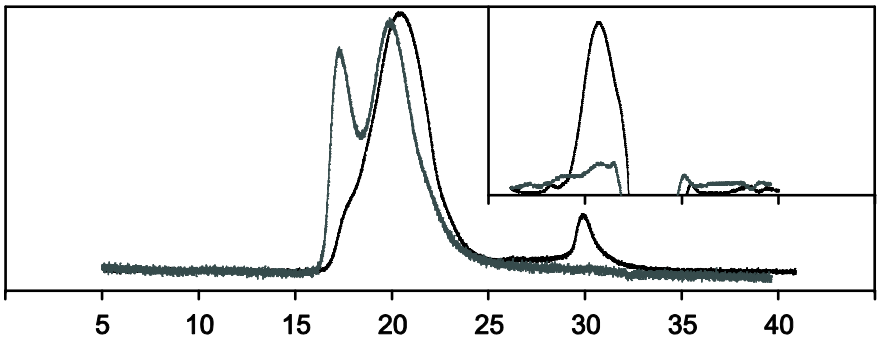

Figure S2.3. LS signals of HA (black) from the reaction mixture before the coupling and HA-(*g*-$M^{NH_2}2005)_{5\%}$ (grey). The inset displays the RI signal in the PAO region of the reaction mixture before and after the coupling.

2.2.2 MALDI-TOF

Solutions for MALDI-TOF analysis were prepared containing; 1) NaTFA (sodium trifluoroacetate) in THF (tetrahydrofurane) (5 mg/ml), 2) DCTB (*trans*-2-[3-(4-*tert*-Butylphenyl)-2-methyl-2-propenylidene]malononitrile) in THF (20mg/ml) and 3) Polyether in THF (10 mg/ml).

20 µl of 2 was mixed with 3 µl of 3 and 1 µl of 1 in the lid of a small phial. Before usage, the pipette was saturated with the fumes of respective solutions. 1 µl of the mixture was added on a metal plate and was allowed to crystallize through evaporation of solvent.

The experiment was performed in linear mode positive with sodium as the cation on a Bruker Daltonics autoflex MALDI-TOF spectrometer (Bruker Daltonics Inc, Billerica, MA, USA). 100 impulses with low laser power were shot on the sample. The data was evaluated using the software programs *Flex analysis* and *Polytools*.

In the following subsections, the molecular weight distribution of the different PAOs is presented. In addition, the molecular weight distribution as obtained using EO or PO as repeating unit are presented. The molecular weight distribution obtained for the PAOs is in general in good agreement with those

obtained from the supplier even though M600 was found to be slightly larger as compared with the product data.

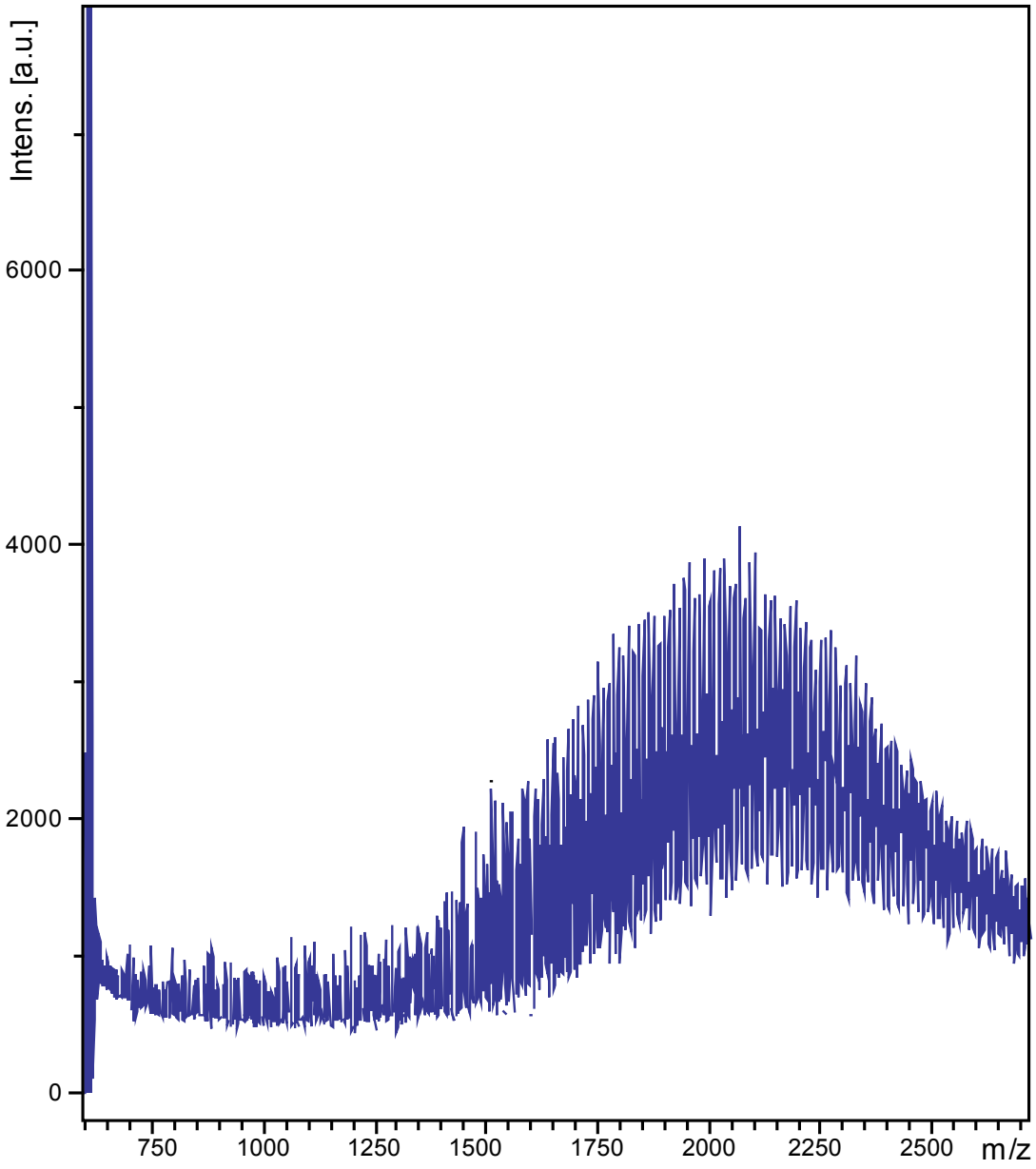

Figure S2.4. $M^{NH_2}2005$ MALDI -TOF results

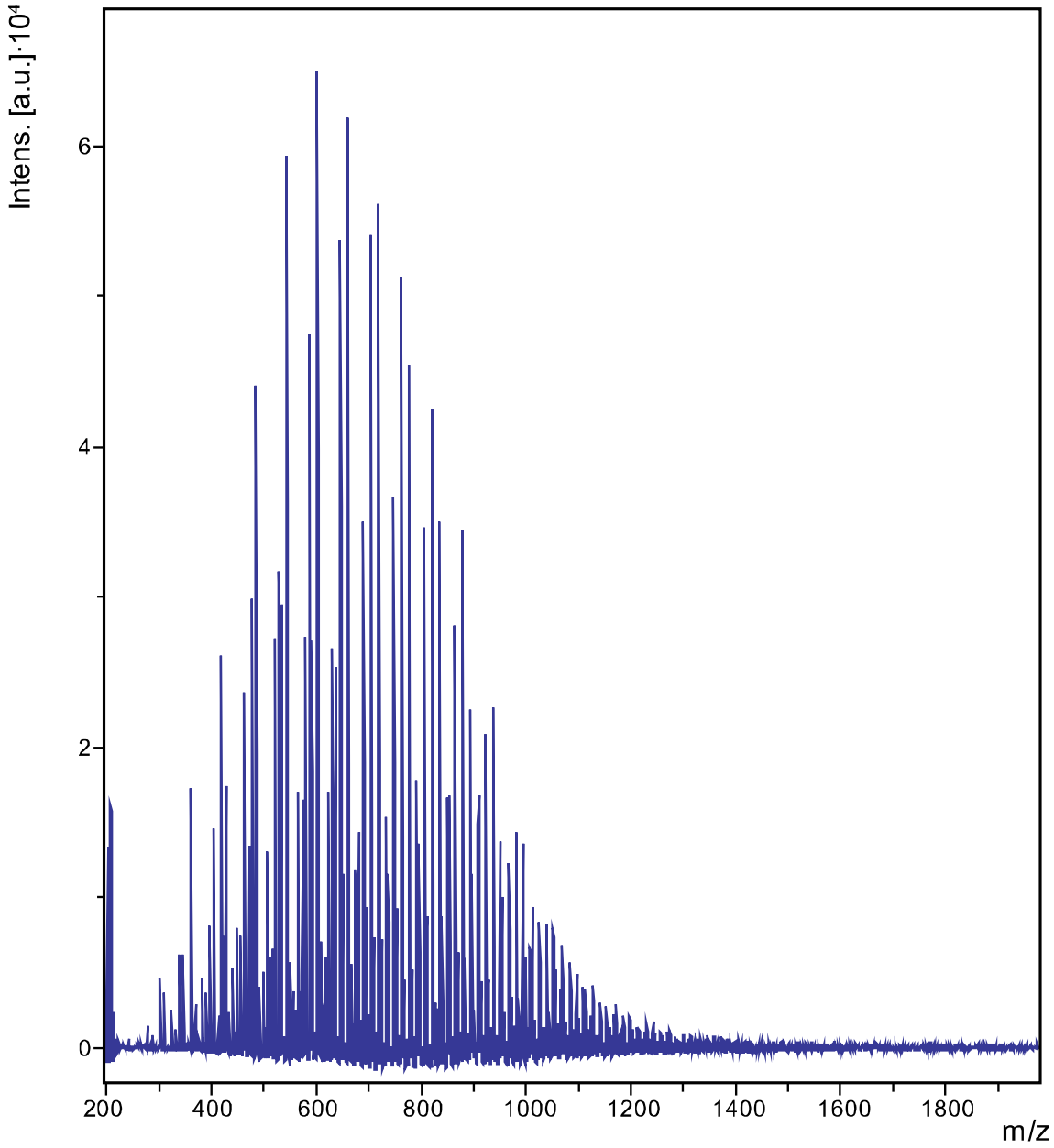

Figure S2.5. $M^{NH_2}600$ MALDI -TOF results

2.2.3 Vibrational spectroscopy

FTIR measurements were performed on KBr tablets with approximately 1/5 polysaccharide derivate using a Perkin Elmer System 2000 FT IR instrument (PerkinElmer Life And Analytical Sciences, Inc, Waltham, MA, USA). The range of the frequency-interval was 4000 – 400 cm^{-1} using 20 scans. All spectra were processed in the software spectrum v2.00. The software Grams was used for resolving bands from the spectra previously obtained.

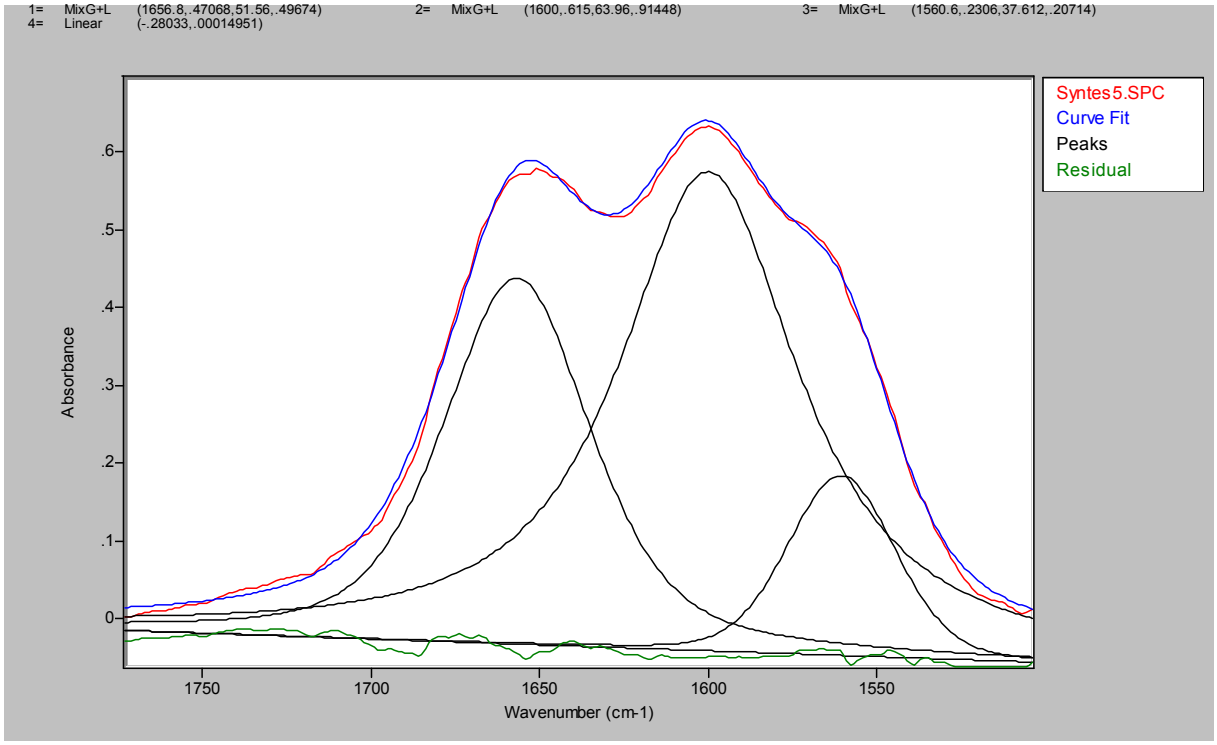

Figure S2.6. Carbonyl region of CMC-(*g*-M^{NH_2}2005)$_{5\%}$

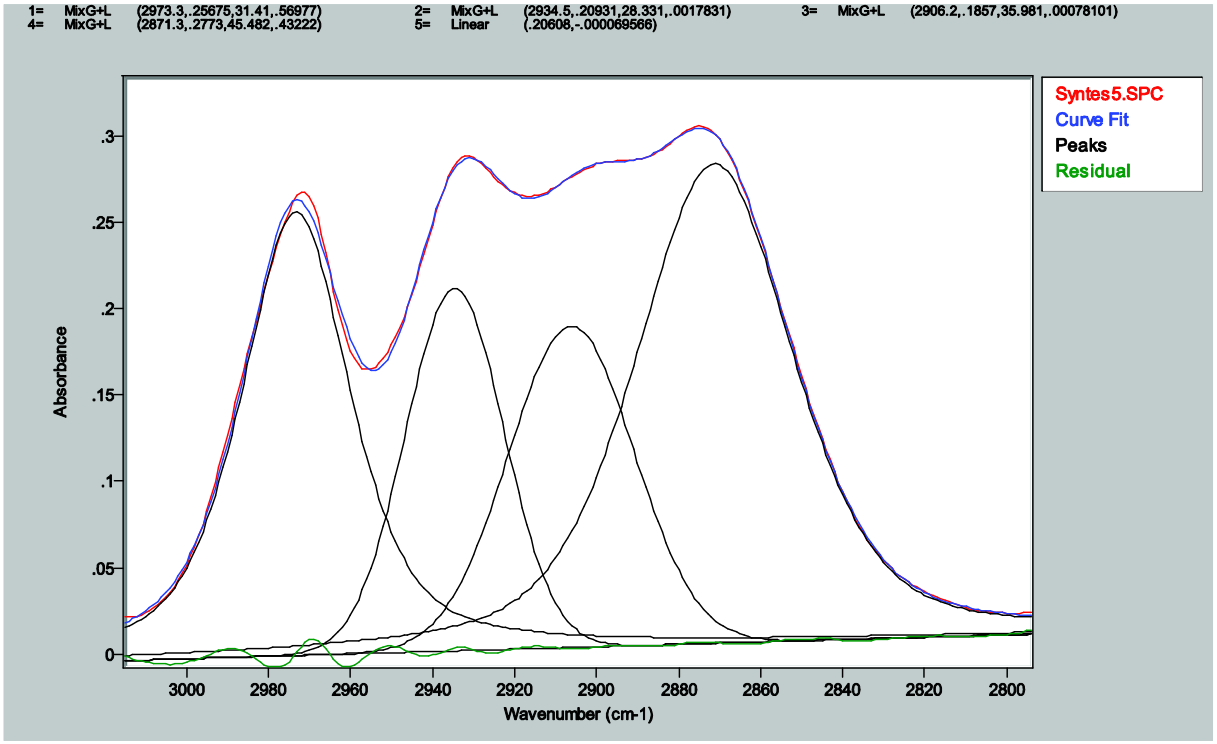

Figure S2.7. Methyl/methylene region of CMC-(*g*-M^{NH_2}2005)$_{5\%}$

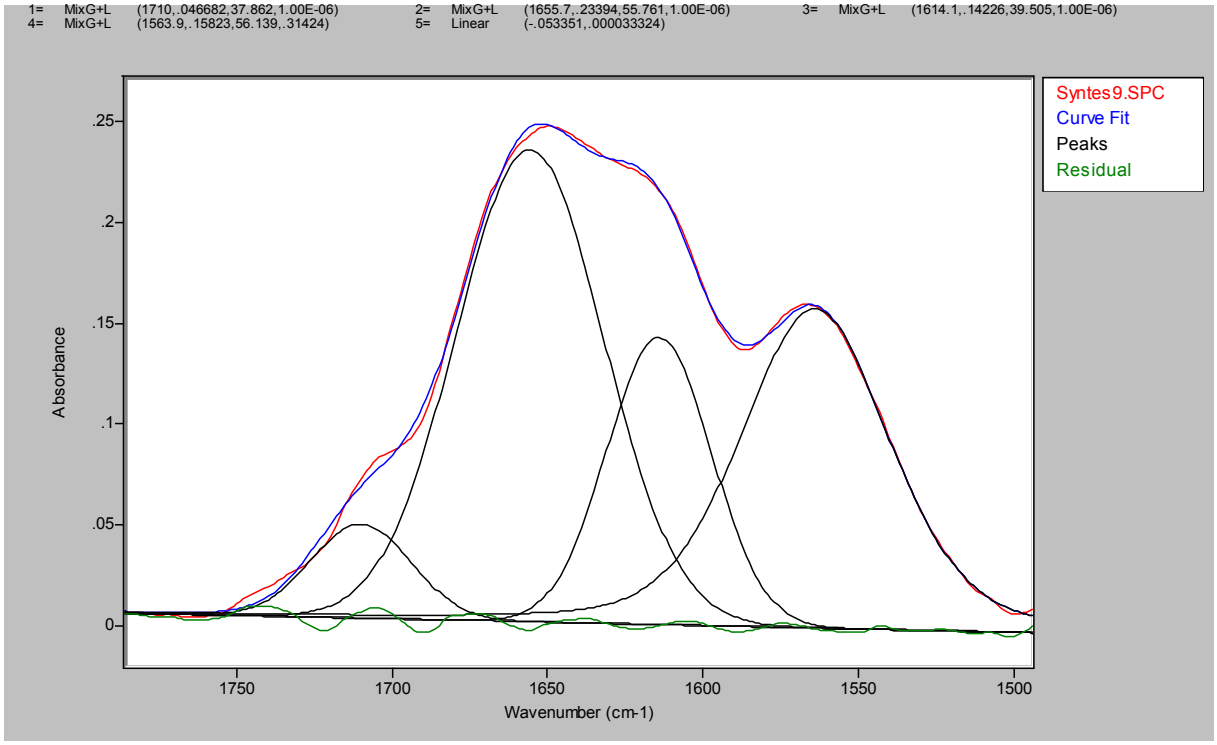

Figure S2.8. Carbonyl region of HA-(*g*-M^{NH_2}2005)$_{5.0\%}$

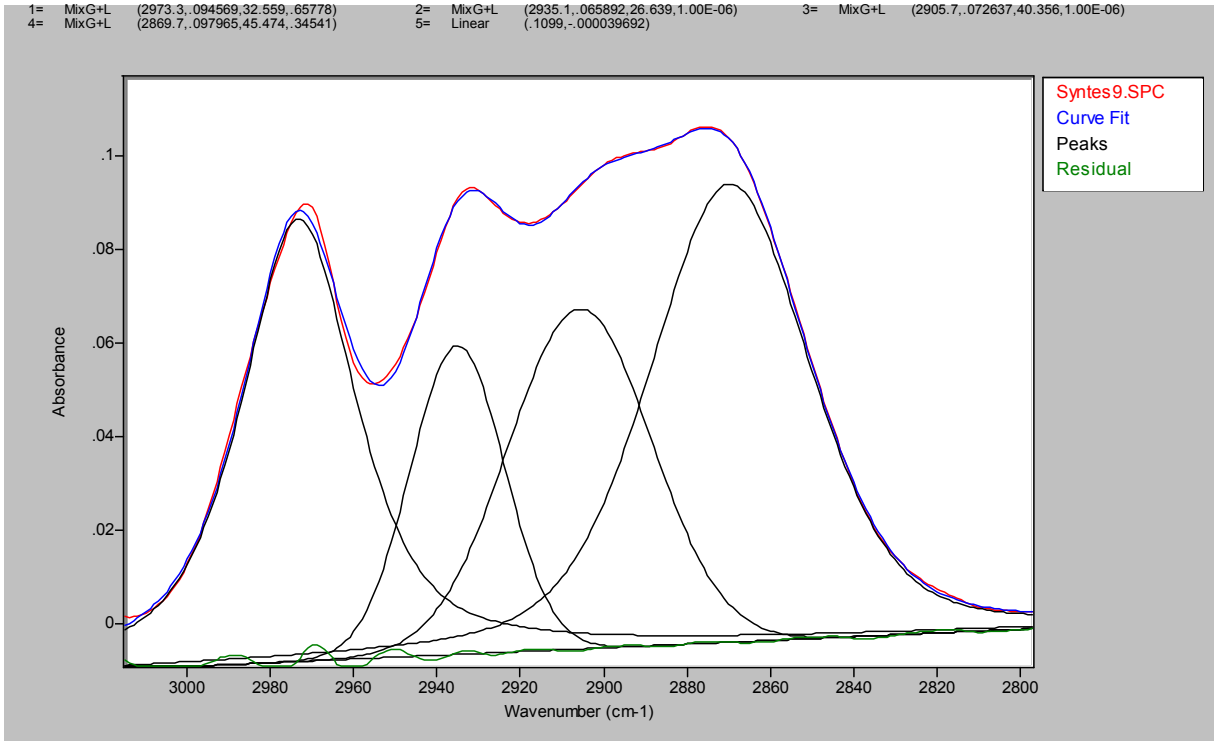

Figure S2.9. Methyl/methylene region of HA-(*g*-M^{NH_2}2005)$_{5.0\%}$

2.2.4 ^{1}H-NMR

The ^{1}H NMR spectra were recorded at ambient temperature (~25°C) on a 300 MHz Varian INOVA 300 (VXR-300) NMR instrument (Vernon Hills, IL, USA). D_2O (99,96 %, Aldrich) was used as solvent for all polymer, poly(alkylene oxide)s and polysaccharides alike except low clouding poly(alkylene oxide)s. Hydrophobic poly(alkylene oxide)s were dissolved in deuterated chloroform (99,8% Aldrich).

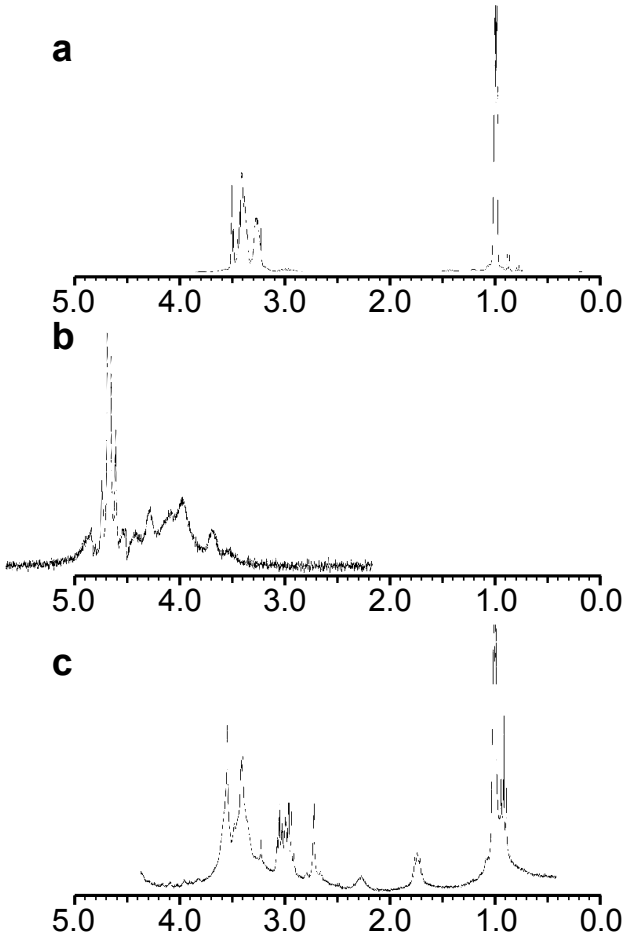

Figure S2.10. ^{1}H-NMR spectra of CMC-(*g*-$M^{NH_2}2005)_{5\%}$.

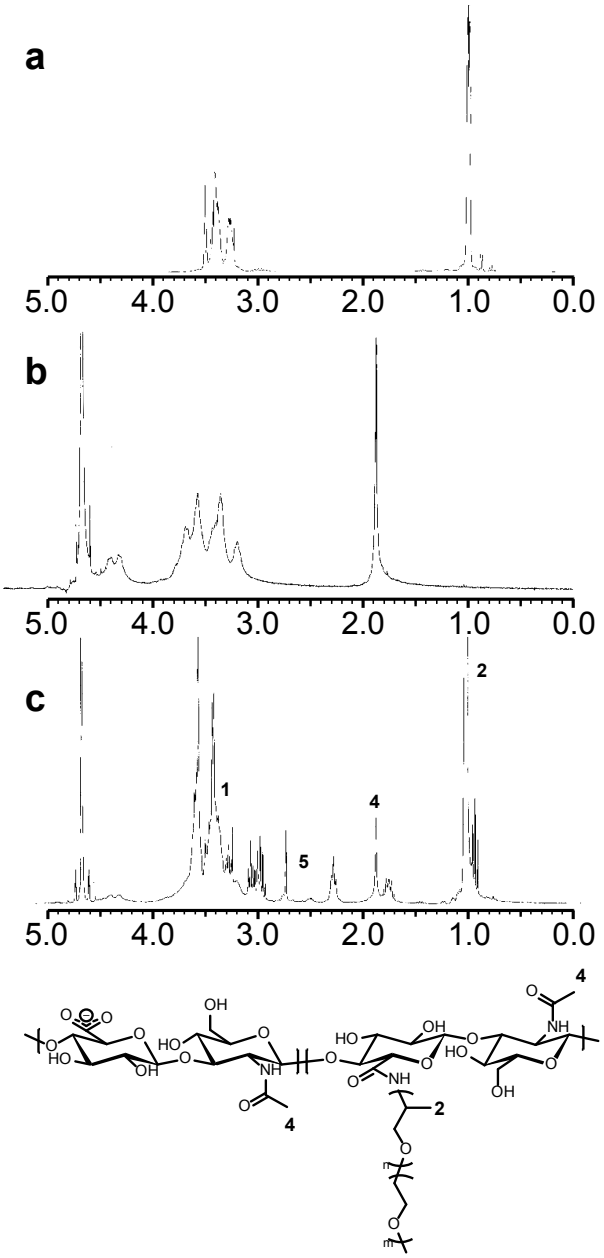

Figure S2.11. ^{1}H-NMR spectra of HA-(*g*-M^{NH_2}2005)$_{10\%}$.

2.2.5 Elemental analysis

Samples were sent to Mikro Kemi AB (Uppsala, Sweden) for CHN and O elemental analysis. The graft ratio was calculated based on the change in carbon content and the results are presented in Table S2.2.

Table S2.2. Synthesis results displayed as the graft ratio φ.

Graft copolymers			Experimental and calculated graft ratio φ [%]		
	Prepolymers				
	PSa	PAO	El[a]	NMR[b]	Theo
CMC-(*g*-$M^{NH_2}2005)_{2.5\%}$	CMC	$M^{NH_2}2005$	2.8		2.5
CMC-(*g*-$M^{NH_2}2005)_{5\%}$	CMC	$M^{NH_2}2005$	5.5		5.0
CMC-(*g*-$M^{NH_2}2005)_{10\%}$	CMC	$M^{NH_2}2005$	10.1		10.0
CMC-(*g*-$M^{NH_2}600)_{17\%}$	CMC	$M^{NH_2}600$	17.5		16.7
CMC-(*g*-$M^{NH_2}600)_{33\%}$	CMC	$M^{NH_2}600$	30.5		33.3
HA-(*g*-$M^{NH_2}2005)_{5.0\%}$	HA	$M^{NH_2}2005$	4.7	5.3	5.0
HA-(*g*-$M^{NH_2}2005)_{10\%}$	HA	$M^{NH_2}2005$	9.6	9.2	10.0

[a]Elemental analysis

[b]NMR quantification of HA based the peak at 1.9 ppm

Abbreviations corresponds to; PAO,=poly(alkylene oxide), PSa=Polysaccharide and Calc corresponds to the hypothetical graft ratio φ, calculated from the starting material in the synthesis procedure, assuming quantitative grafting.

3 Thermodynamic considerations

3.1 van't Hoff relation

The molar fraction for free and grafted polyether chains x_C has been expressed in terms of the moles of the (average) monomers of M2005. The standard free energy $\Delta G°c$ for the transfer of 1 mole of PAO monomer from the solution to the phase separated/micellar phase at the critical point is expressed according to Equation S1[2].

$$\Delta G^\circ_c = RT\ln(c) \quad \text{S1}$$

Applying the Gibbs-Helmholtz relationship, the standard enthalpy change for association can be expressed according to Equation S2.

$$\Delta H^\circ_c = -RT^2\left[\frac{\partial \ln(c)}{\partial T}\right]_P \quad \text{S2}$$

The standard entropy change is subsequently expressed according to Equation S3.

$$\Delta S^\circ_c = \frac{\left(\Delta H^\circ_c - \Delta G^\circ_c\right)}{T} \quad \text{S3}$$

To obtain the standard enthalpy change, the T_{ass} and T_{cp} curves were fitted with logarithmic functions (see Figure S3.1) in order to obtain accurate values of the derivative in Equation S2.

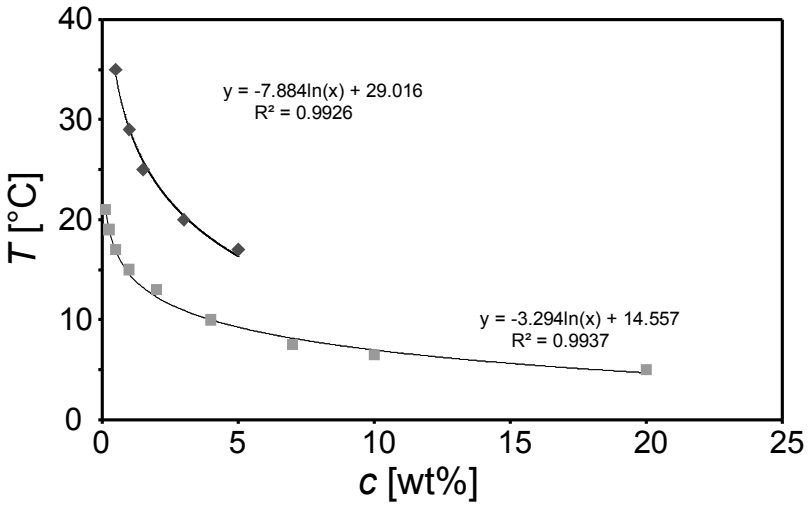

Figure S3.1. Logarithmic curve fitting for T_{ass} and T_{cp}.

The gelation line in Fig. 8b in the article was obtained and used in the same manner as above to extract the thermodynamic parameters in Table S3.1. The data points used for the construction of the phase line included all definitions for the gel point. The data points for the high thermogelling region were not

included. For HA-(g-M^{NH2}2005)$_{10\%}$, both the gelation and the phase transition into the high thermogelling region coincide, however this is not necessarily the case for CMC-based derivatives.

Table S3.1. Thermodynamic parameters at different temperatures for HA-(g-M^{NH2}2005)$_{10\%}$.

T	c [mol %]			ΔG [kJ/mol]			ΔH [kJ/mol]			ΔS [kJ/mol/K]		
	c_{cp}	c_{ass}	c_{gel}	ΔG_{cp}	ΔG_{ass}	ΔG_{gel}	ΔH_{cp}	ΔH_{ass}	ΔH_{gel}	ΔS_{cp}	ΔS_{ass}	ΔS_{gel}
20	$2.5\cdot10^{-05}$	$9.1\cdot10^{-03}$	1.0	-25.8	-11.5	-0.1	-12.1	-28.9	-14.4	1514.0	-18.2	-0.7
22	$1.4\cdot10^{-05}$	$7.0\cdot10^{-03}$	0.32	-27.5	-12.2	-2.8	-14.5	-34.7	-17.3	1853.2	-70.6	-0.6
25	$7.5\cdot10^{-06}$	$5.4\cdot10^{-03}$	0.15	-29.1	-12.9	-4.7	-17.1	-41.0	-20.4	2221.9	-185.8	-0.6
30	$1.7\cdot10^{-06}$	$2.9\cdot10^{-03}$	0.034	-33.4	-14.7	-8.5	-24.6	-59.0	-29.4	3080.9	-1284.4	-0.7
35	$3.6\cdot10^{-07}$	$1.5\cdot10^{-03}$	$9.2\cdot10^{-03}$	-37.9	-16.6	-12.0	-33.5	-80.3	-40.1	2863.6	-6934.3	-0.8

3.2 Phase diagram. v_0 and τ

In this section. the evolution of the material properties (zero shear viscority. relaxation time. shear moduli) as a function of temperature and concentration will be discussed and theoretically investigated within the framework of phase diagrams and simple solution theory. Let as consider a generic LCST phase diagram as in Figure S3.2.

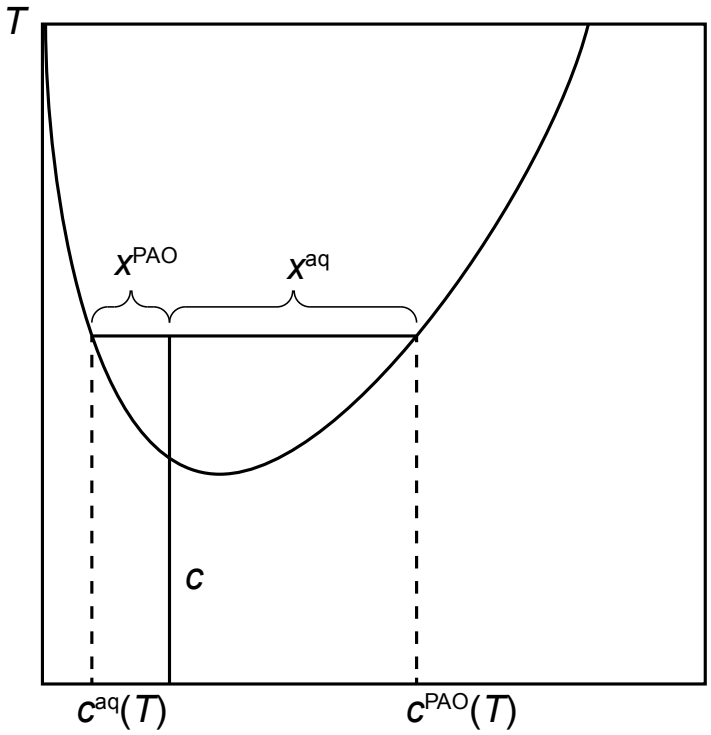

Figure S3.2. Phase diagram.

For a given graft copolymer concentration. increasing the graft ratio φ. corresponds to increasing the global PAO concentration c. i.e. moving from right to left on the x-axis. The number of cross-linking domains v_0 should be proportional to the molar fraction PAO x^{PAO} residing in the PAO-rich phase.

$$\nu_0(c) \propto x^{PAO}(c) \quad \text{S4}$$
$$\varphi \propto c$$

The fraction can be obtained using the Lever rule.

$$x^{PAO}(c) = \frac{c - c^{aq}(T)}{c^{PAO}(T) - c^{aq}(T)} \quad \text{S5}$$

Clearly. υ_0 scales with c which is also observed in the article as η_0 scales with φ.

In the article. we argue that $\upsilon_0(T)$ remains constant as a function of T. Using the same argumentation as above. $x^{PAO}(T)$ being constant as a function of T is only possible for a perfectly symmetric binodal curve which is certainly not the case. For this relationship to hold. ν_0 must consequently be more or less independent of temperature. A common misconception is that ν_0 indicates the number of grafts or sticky groups. However. ν_0 is a measure of the number of macromolecules with at least two stickers (i.e. PAO grafts) in different aggregates. Since the number of grafts per copolymer chain discussed in this paper is approximately between 50-150. it can be assumed that all chains have grafts participating in different microdomains. Consequently. ν_0 is more or less constant whereas the fraction of grafts participating in microdomains as the aggregation number increases with temperature. To summarize. for graft copolymers with a sufficiently high graft ratio. η_0 is primarily determined by τ. and ν_0 is more or less temperature independent.

Let us now consider the evolution of N_{agg} as a function of temperature. We can assume that

$$N_{agg} \propto c^{PAO}(T) \quad \text{S6}$$

At the binodal curve. the chemical potential of the components is zero

$$\mu_{PAO} - \mu_{PAO}^{\circ} \cong RT\left[ln\left(c^{PAO}\right)\right] \quad \text{S7}$$
$$\mu_{PAO} = 0 \quad \text{S8}$$
$$ln\left(c^{PAO}\right) = \frac{-\mu_{PAO}^{\circ}}{RT} \quad \text{S9}$$
$$c^{PAO} = e^{\frac{-\mu_{PAO}^{\circ}}{RT}}$$

Note that Equations S7-S9 are essentially equivalent to Equation S1. Therefore

$$N_{agg} \propto \exp\left[\frac{-\mu_{PAO}^{\circ}}{RT}\right] \quad \text{S10}$$

which is a temperature dependence often reported for non-ionic surfactants based on PEO. By combining Equation S10 with the temperature dependence of τ and η_0 (see the article) in the high segregation regime with an activation energy E_a^{high}. one obtains

$$\tau \propto N_{agg}^{3/2} \exp\left[\frac{E_a^{high}}{RT}\right] = \exp\left[\frac{2E_a^{high} - 3\mu_{PAO}^{\circ}}{2RT}\right] \quad \text{S11}$$

Note that is E_a^{high} negative. In the high segregation regime. all PAO grafts have phase separated into microdomains and

$$\tau \propto \exp\left[\frac{E_a^{high}}{RT}\right] \quad \text{S12}$$

Therefore. it follows that

$$\eta_0(T) \propto v_0(T)\tau(T) \propto v_0\tau(T) \quad \text{S13}$$

4 Rheology

In the following sub-sections. complementary flow curves. master curves and the evolution of viscoelastic parameters as a function temperature are presented. In addition. the signs of the phenomena shear-banding is presented and discussed.

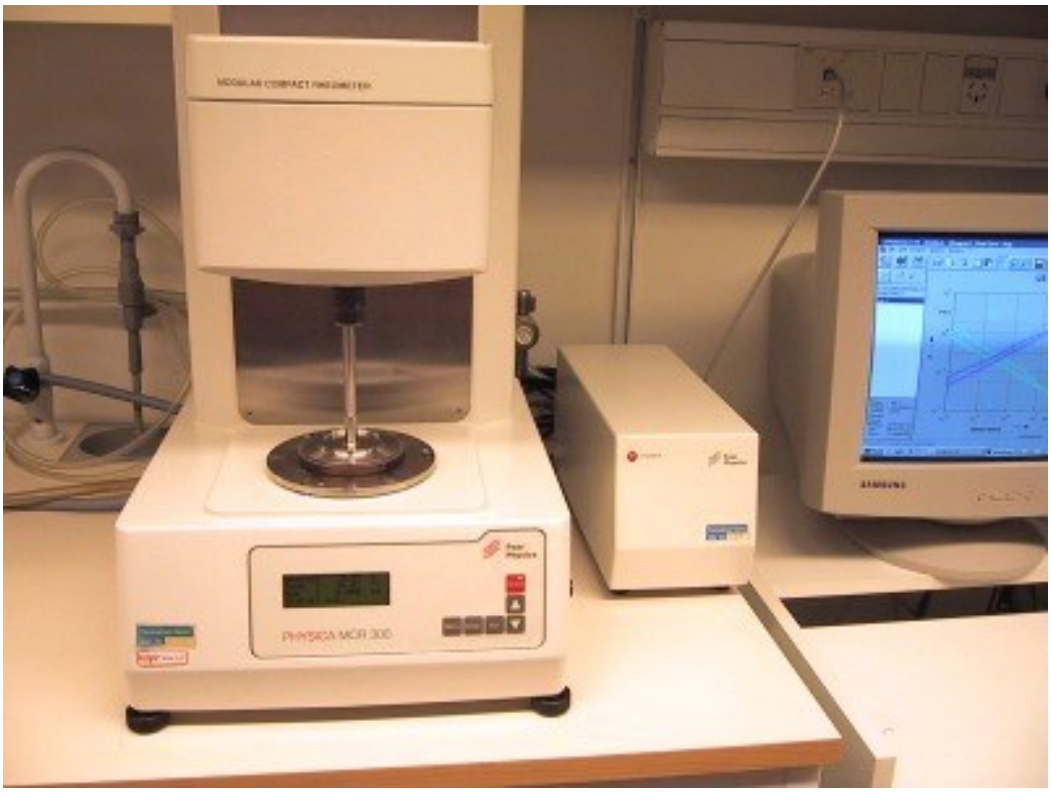

Figure 4.1. Paar Physica. MCR 300 Universal Rheometer.

4.1 Flow curves

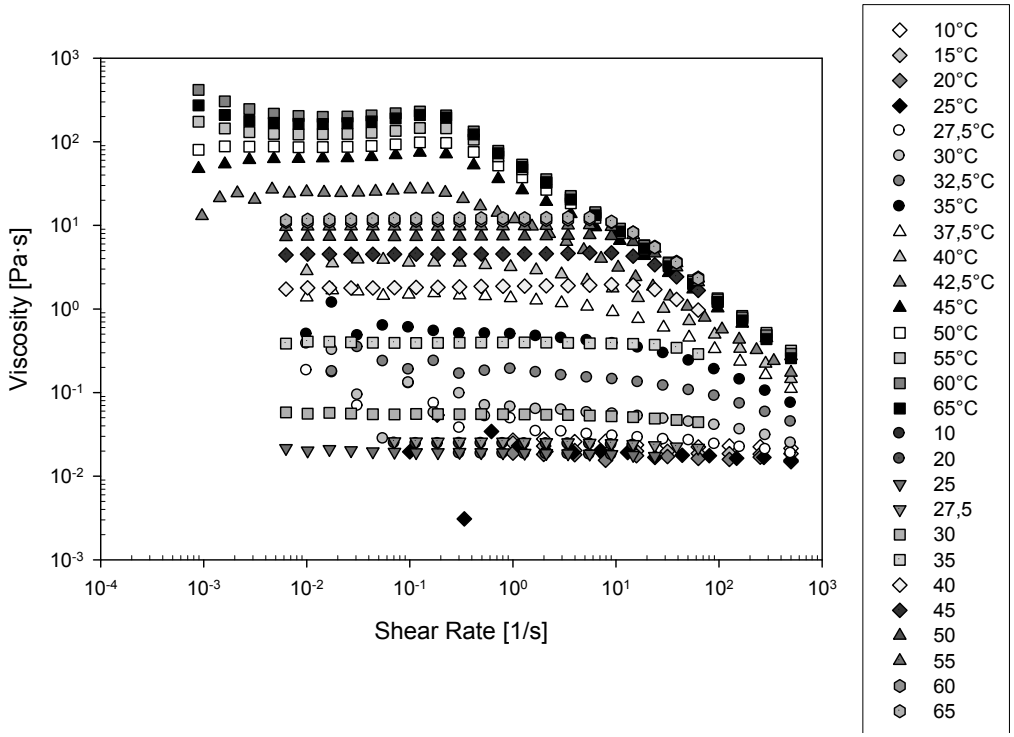

Figure S4.2. Complex viscosity and shear viscosity for HA-(*g*-$M^{NH2}2005)_{10\%}$. 3 wt%. The top legends ranging from 10 to 65 °C correspond to the steady shear rheometry and the bottom legends ranging from 10 to 65 °C correspond to the complex viscosity obtained from oscillatory rheometry.

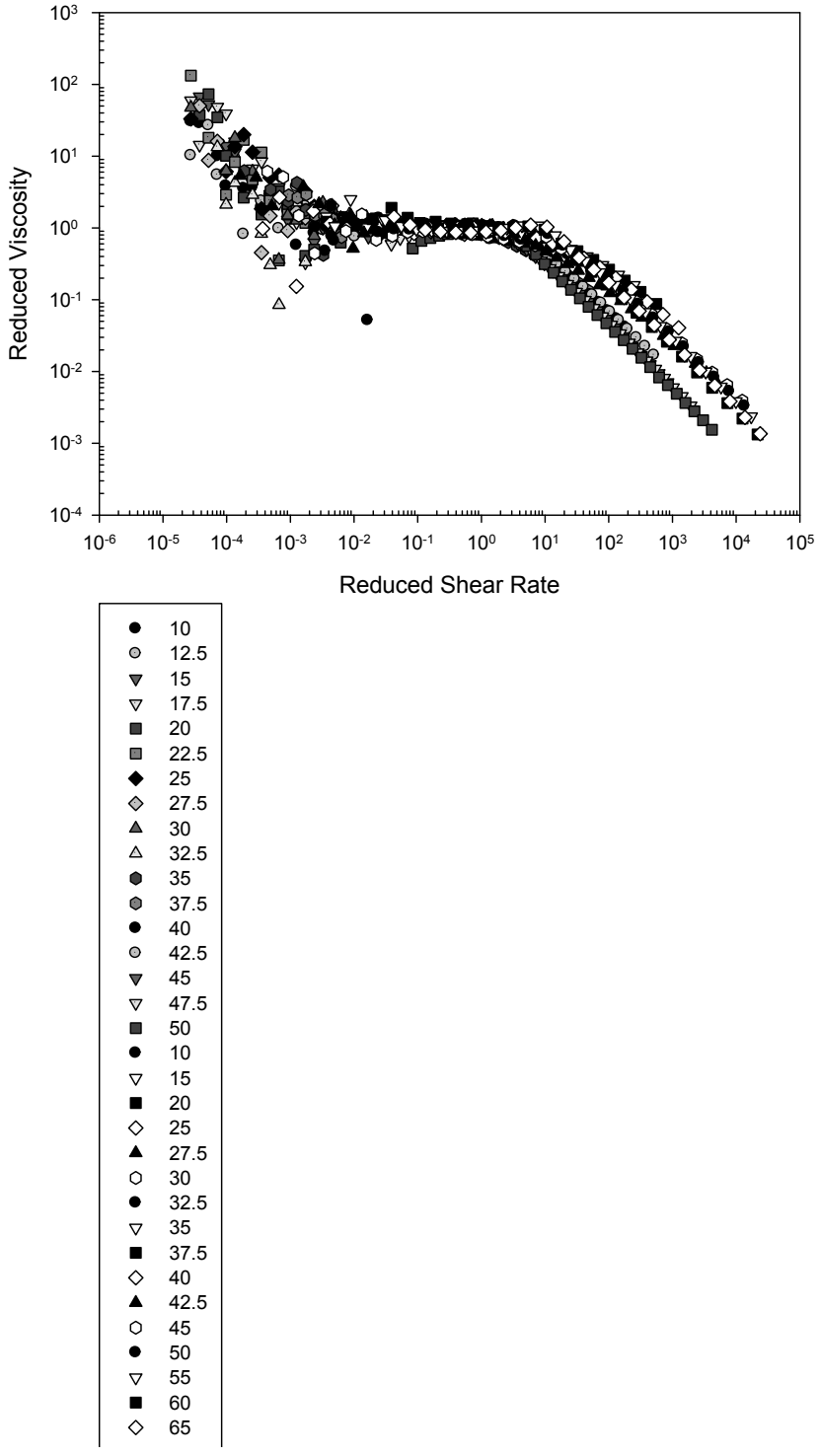

Figure S4.3. Master (flow) curve for CMC-(*g*-$M^{NH2}2005)_{5\%}$. 3 wt% (top legends) and HA-(*g*-$M^{NH2}2005)_{10\%}$. 3 wt% (bottom legends) corresponding to the reduced viscosity as a function of the reduced shear rate. The reduced parameters have been obtained using the data points in Figure 3 in the article**.**

4.2 Strain-hardening and shear-thickening

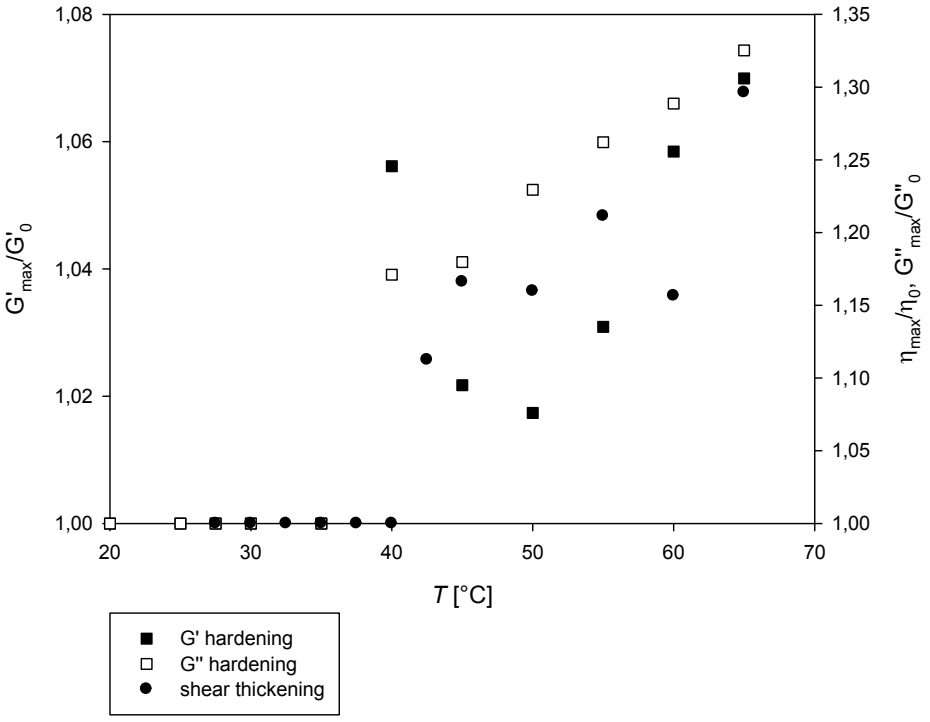

Figure S4.4. Strain-hardening and Shear-thickening for HA-(*g*-$M^{NH2}2005)_{10\%}$. 3 wt%.

4.3 Oscillatory frequency dependence

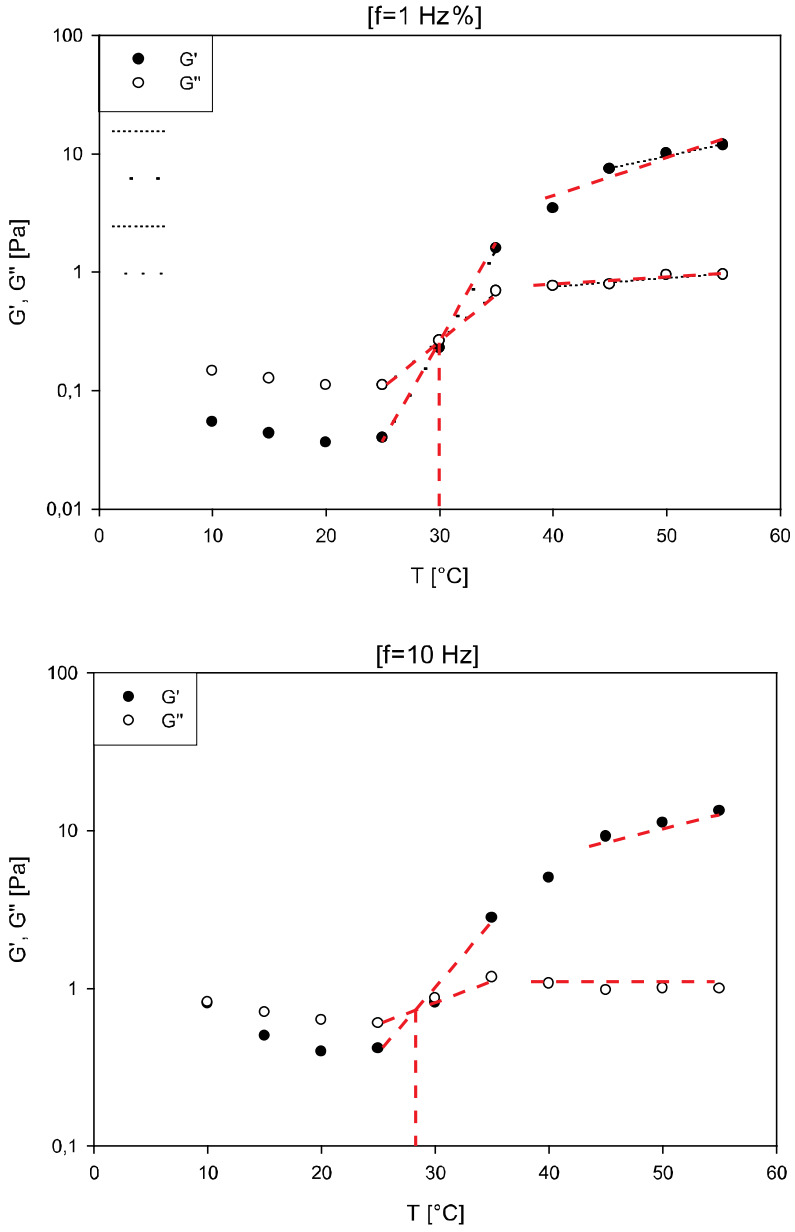

Figure S4.5. Evolution of G' and G'' and their intersection as a function of temperature at f=1 Hz and f=10 Hz for CMC-(*g*-$M^{NH2}2005)_{10\%}$. 1 wt%.

The gel formation is displayed for different graft copolymers in Figure S4.6. Figure S4.7 and Figure S4.8. At high temperatures. the gel can be defined as a solid gel or approaches properties corresponding to a viscoelastic solid. Note that CMC-based graft copolymers are already in a gel state below the association temperature.

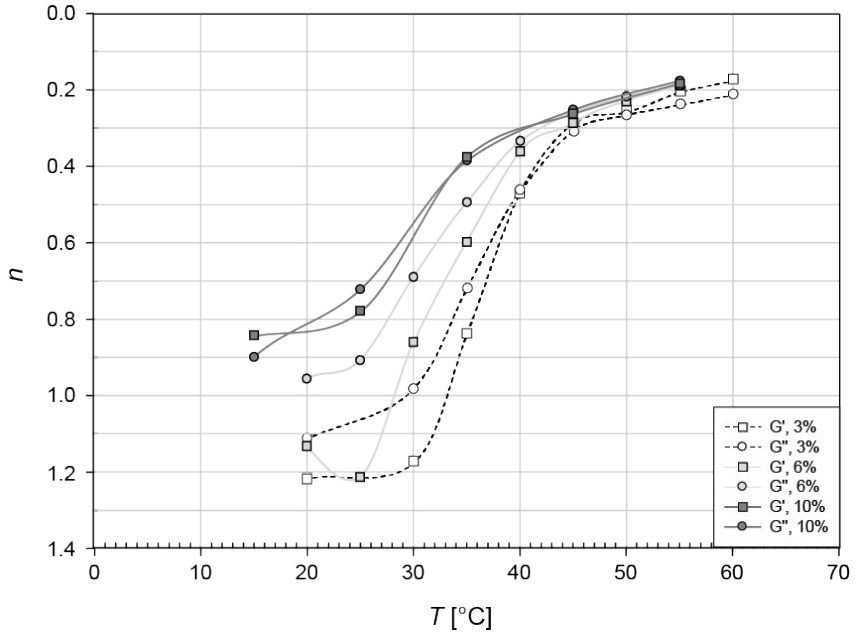

Figure S4.6. Exponent n of $G'=\omega^{n'}$ (open symbol) and $G''=\omega^{n''}$ (closed symbol) as a function of temperature for 3. 6 and 10 wt% HA-(g-M^{NH2}2005)$_{10\%}$.

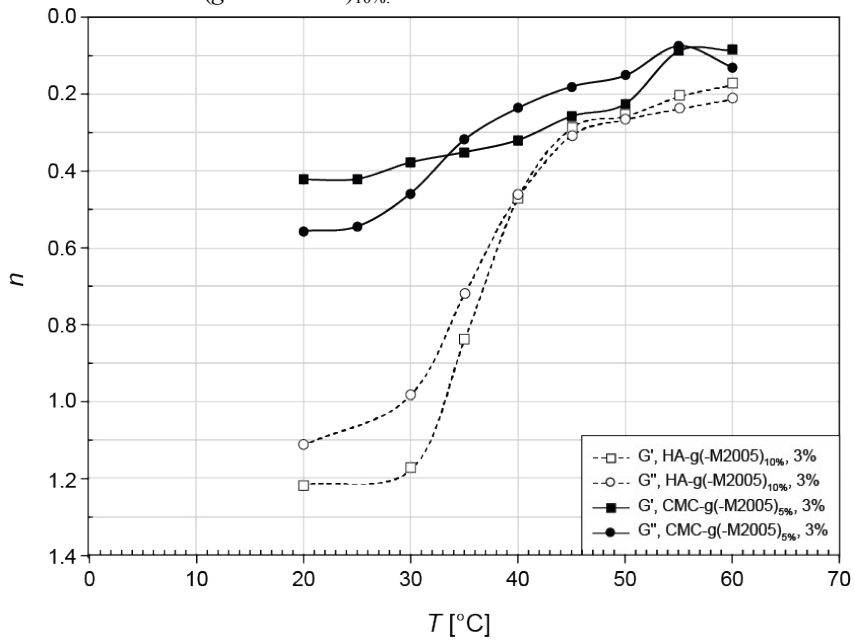

Figure S4.7. Exponent n of $G'=\omega^{n'}$ (open symbol) and $G''=\omega^{n''}$ (closed symbol) as a function of temperature for 3. wt% HA-(g-M^{NH2}2005)$_{10\%}$ and CMC-(g-M^{NH2}2005)$_{5\%}$.

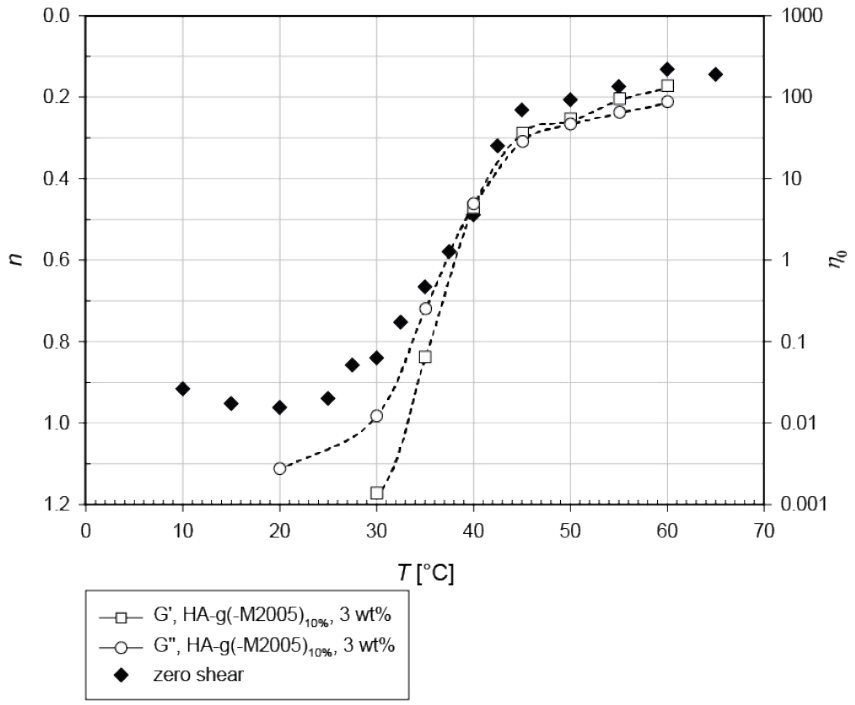

Figure S4.8. Exponent n of $G'=\omega^{n'}$ (open symbol) and $G''=\omega^{n''}$ (closed symbol) and the zero shear viscosity η_0 as a function of temperature for 3. wt% HA-(g-M^{NH2}2005)$_{10\%}$.

The temperature regimes observed for the zero shear viscosity are also clearly observed when inspecting the evolution of the exponent n as a function of temperature.

The strength of the network in the respective temperature regimes were investigated by stress relaxation ($G(t) = t^{-\Delta}$) measurements by Aubry et al. It was found that the low temperature regime corresponds as a soft critical gel with a high network specific exponent Δ . whereas the high temperature regime corresponds to a stiff critical gel with a low network specific exponent Δ[3]. In our work. it was detected that the threshold gel point was always in the low temperature regime regarding CMC derivates and shifted toward the onset of the high temperature regime regarding the HA derivates. The discrepancy between the two polysaccharide derivates is simply explained by the intrinsic elastically properties of the CMC backbone.

4.4 Shear-banding

It is clear that the graft copolymer solutions develop into very strong gels at elevated temperatures. especially for higher graft copolymer concentrations (Figure S4.9). The strong gel structure due to the strong cross-linking junctions is most likely the explanation for the phenomena shear-thickening (Figure S4.10) as well as shear-banding (Figure S4.11). The indications for shear banding are observed at

elevated temperature and for high graft copolymer concentrations (6 and 10 wt% in Figure S4.11) by plateaus and maxima in the strain-stress curves (marked by red circles). It is plausible that the shear-banding results in two distinct gel structure. one in the bottom with maintained strong cross-linking junctions that is relatively immobile and one with disrupted junctions close to the cone that is relatively easily deformed by the shearing.

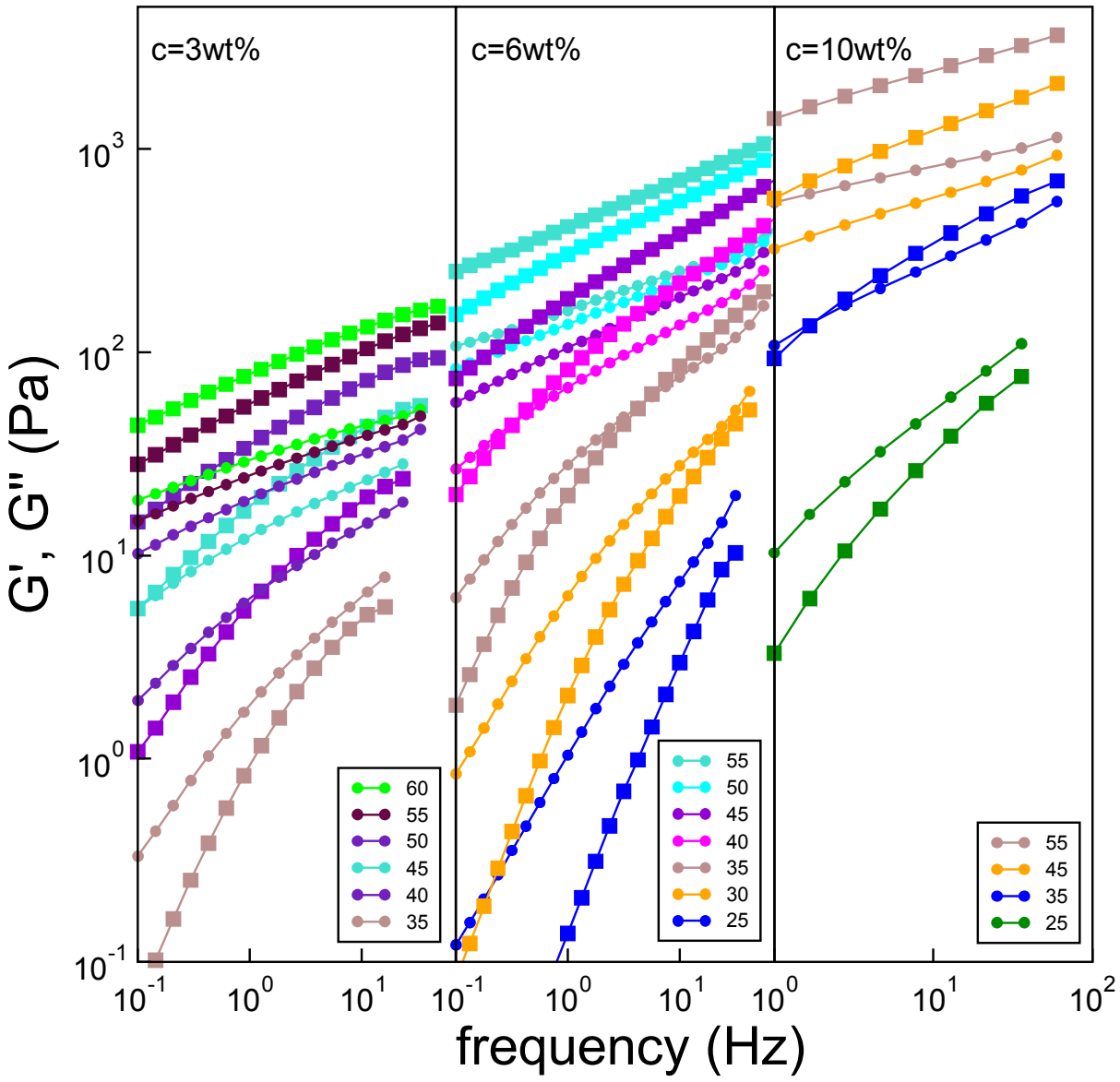

Figure S4.9. *G′* (squares) and *G″* (circles) as a function of frequency and temperature for 3. 6 and 10 wt% HA-(*g*-$M^{NH2}2005)_{10\%}$.

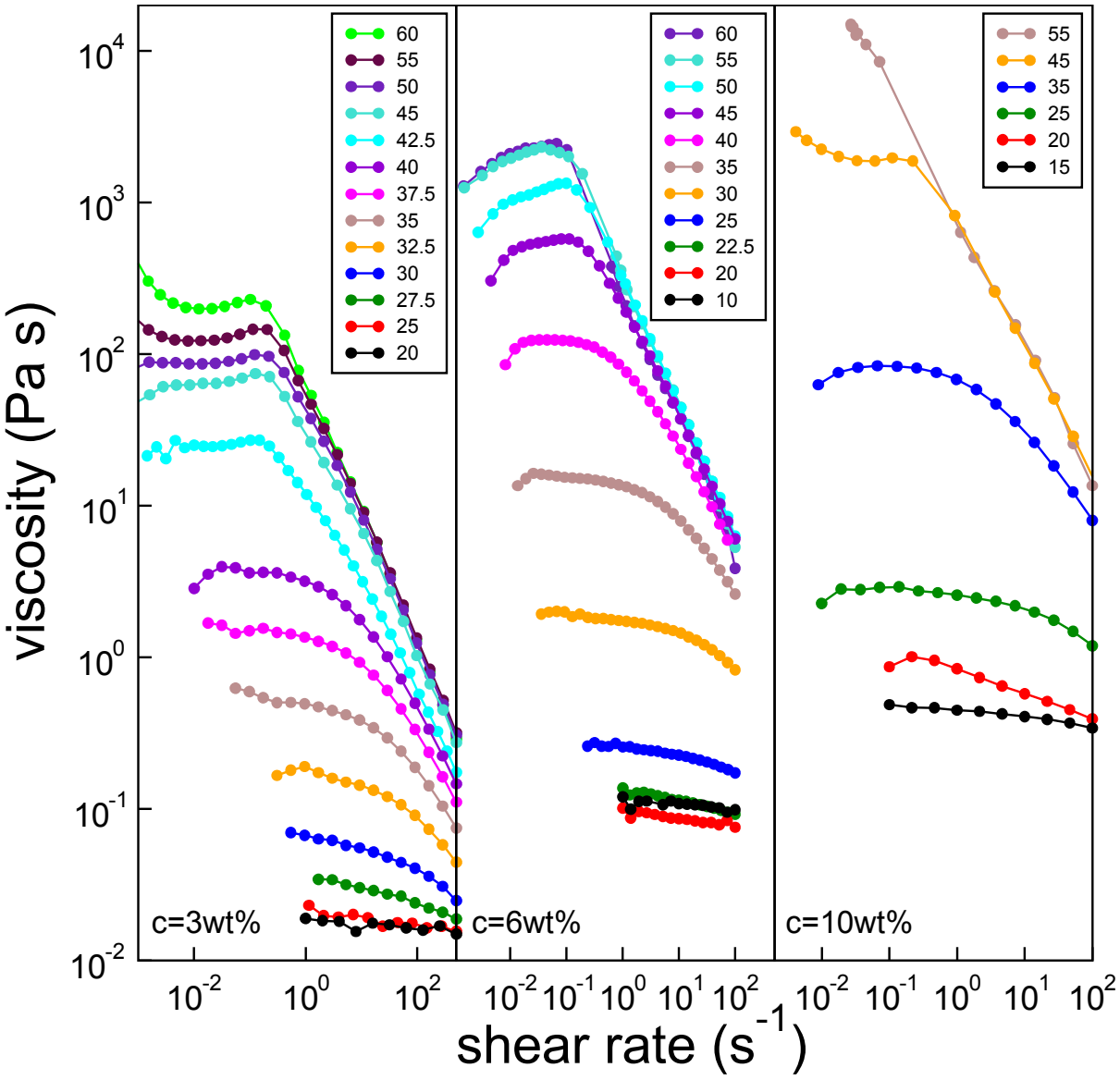

Figure S4.10. Flow curves at different temperatures for 3. 6 and 10 wt% HA-(*g*-$M^{NH2}2005)_{10\%}$.

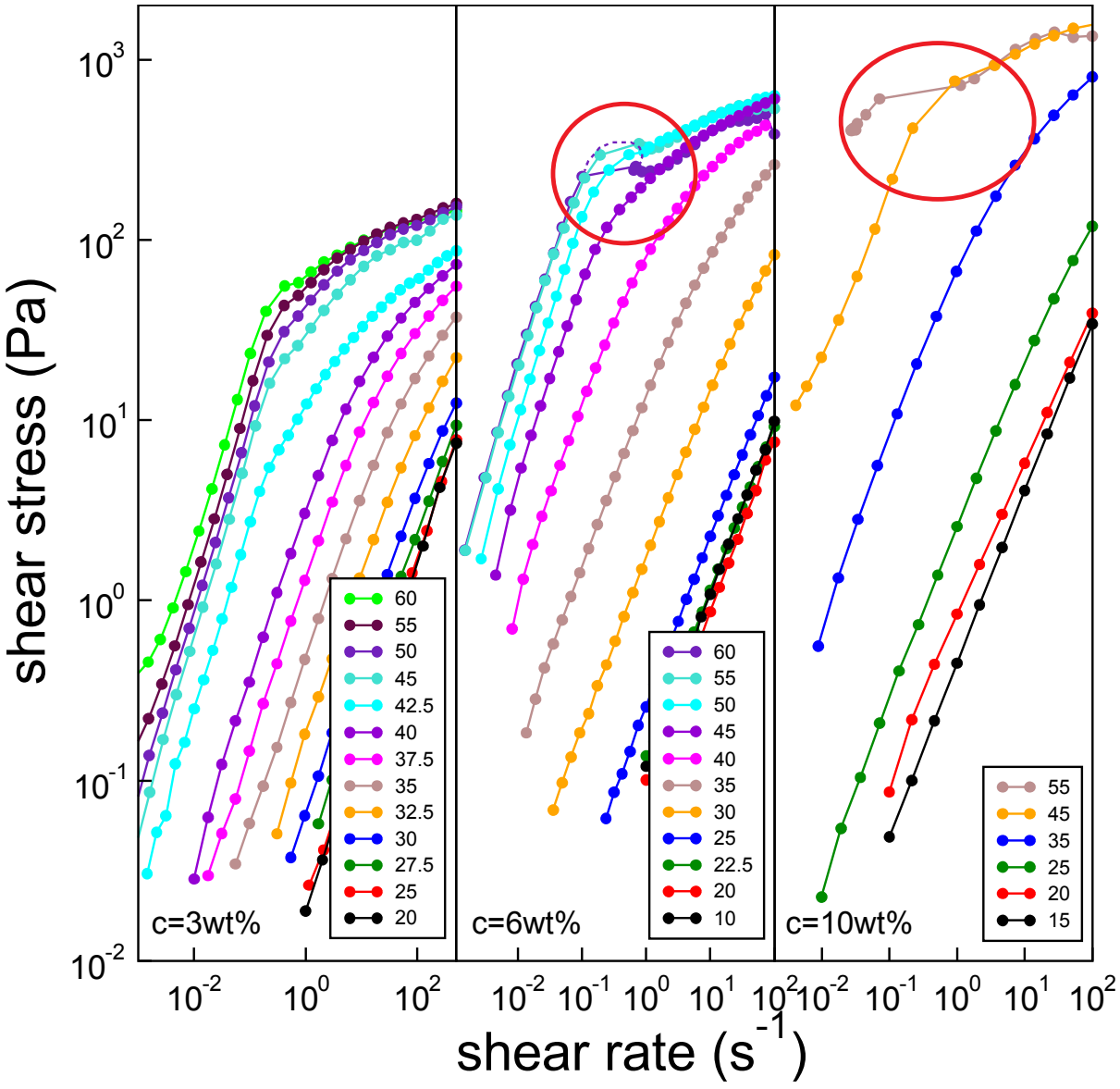

Figure S4.11. Stress-strain curves at different temperatures for 3. 6 and 10 wt% HA-(*g*-M^{NH2}2005)$_{10\%}$.

5 References

(1) Andersson Trojer. M.; Andersson. M.; Bergenholtz. J.; Gatenholm. P. Quantitative grafting for structure-function establishment: Thermoresponsive poly(alkylene oxide) graft copolymers based on hyaluronic acid and carboxymethylcellulose. *Biomacromolecules* **2019.** *20*. 1271-1280.
(2) Alexandridis. P.; Holzwarth. J. F.; Hatton. T. A. Micellization of Poly(ethylene oxide)-Poly(propylene oxide)-Poly(ethylene oxide) Triblock Copolymers in Aqueous Solutions: Thermodynamics of Copolymer Association. *Macromolecules* **1994.** *27*. 2414-2425.
(3) Aubry. T.; Bossard. F.; Staikos. G.; Bokias. G. Rheological study of semidilute aqueous solutions of a thermoassociative copolymer. *Journal of Rheology* **2003.** *47*. 577-587.